Dalitz-plot binning optimization for measuring the CKM angle β

A model-independent approach to
$B^0 \to D\pi^+\pi^-$, $D \to K^0_S\pi^+\pi^-$

Anfeng Li
Tsinghua University
With W. Qian, B. Shi, A. Xu and L. Zhang

5 November 2026 | A. Li et al., arXiv:2610.15839

Outline

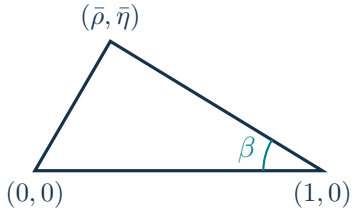
1. Physics motivation
2. Binned Dalitz formalism
3. Binning optimization
4. Results and validation
5. Summary and outlook

CKM angle β

The CKM matrix describes quark mixing. Its complex phase permits CP violation.

$$\beta \equiv \arg\left[-\frac{V_{cd}V_{cb}^*}{V_{td}V_{tb}^*}\right].$$

- $B^0 \to J/\psi K_S^0$ gives a precise reference through $\sin 2\beta$.
- Tree-level $b \to c\bar{u}d$ decays have no penguin contribution to the decay amplitude.
- The decay-chain interference is sensitive to both $\sin 2\beta$ and $\cos 2\beta$.

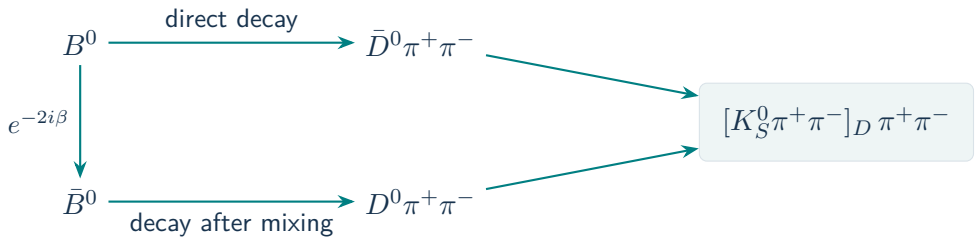


The Unitarity Triangle (schematic)

$B^0 \to D\pi^+\pi^-$ offers a charged-track final state when $D \to K_S^0\pi^+\pi^-$ and $K_S^0 \to \pi^+\pi^-$.

Bondar, Kuzmin, Vorobyev, JHEP 03 (2018) 195; Frings, Nierste, Wiebusch, Phys. Rev. Lett. 115 (2015) 061802.

Mixing-induced CP violation



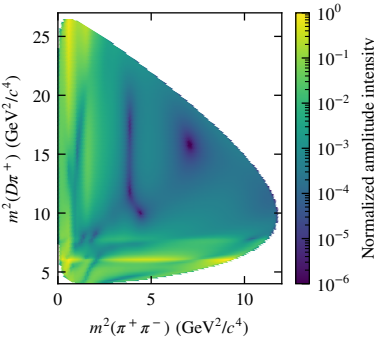
$$\mathcal{A}(t) \propto A_1 \cos\frac{\Delta m_B t}{2} + i\, e^{-2i\beta} A_2 \sin\frac{\Delta m_B t}{2}.$$

A_1 and A_2 describe the two decay chains; Δm_B is the oscillation frequency.

The two paths reach the same final state. Their interference depends on both the weak phase 2β and the strong phases of the decay amplitudes.

Bondar, Kuzmin, Vorobyev, JHEP 03 (2018) 195. Common exponential decay factor omitted; leading decay amplitudes shown.

Dalitz-plot structure



Two coordinates for a three-body decay

- Each event is a point in the two-dimensional phase space.
- Resonances create structure in the amplitude magnitude and phase.
- The colour shows the model intensity on a logarithmic scale.

An unbinned amplitude analysis describes this variation with a Dalitz-plot amplitude model. A binned analysis can instead use measured bin integrals.

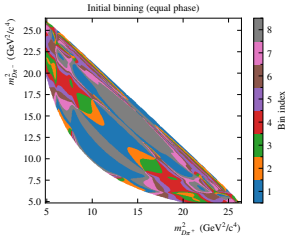
Figure: A. Li et al., arXiv:2610.15839, Fig. 1 (left panel). Model: LHCb, Phys. Rev. D 92 (2015) 032002.

Outline

1. Physics motivation
2. Binned Dalitz formalism
3. Binning optimization
4. Results and validation
5. Summary and outlook

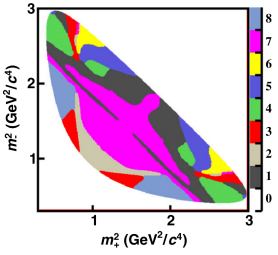
Binned double-Dalitz analysis

$B^0 \to D\pi^+\pi^-$: B **bins** j



$j = \pm 1, \ldots, \pm\mathcal{M}, \quad \mathcal{M} = 8$ pairs.
Equal-phase starting point; **bins optimized**.

$D \to K^0_S\pi^+\pi^-$: D **bins** i



$i = \pm 1, \ldots, \pm\mathcal{N}, \quad \mathcal{N} = 8$ pairs.
Established scheme; **bins held fixed**.

$\mu^2_\pm = m^2(D\pi^\pm)$, $m^2_\pm = m^2(K^0_S\pi^\pm)$. Reflected bin partners share a colour.

Each event provides a bin pair (j, i), a decay time t and an initial-flavour tag q.

Method: Bondar, Kuzmin, Vorobyev, JHEP 03 (2018) 195. B map: A. Li et al., arXiv:2610.15839, Fig. 3(b), left panel.

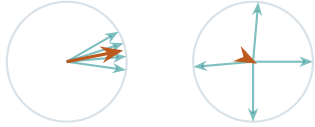
Binned hadronic parameters

B bins	D bins	Physical meaning
k_j	K_i	Relative populations of flavour-specific decays
c_j, s_j	C_i, S_i	Strong-phase information retained within a bin

$$c_j + is_j = \frac{\int_{\mathcal{B}_j} |A_B|\,|\bar{A}_B|\, e^{i\Delta\delta_B}\,\mathrm{d}\Phi}{\sqrt{k_j k_{-j}}}.$$

$\Delta\delta_B = \arg \bar{A}_B - \arg A_B$: strong-phase difference between the two B decay paths.

c_j, s_j: normalized integrals of the amplitude-weighted cosine and sine.



Similar phases Varying phases

Phase variation within a bin can cancel interference: $c_j^2 + s_j^2 \leq 1$.

B parameters can be fitted together with β. External D strong-phase inputs are measured using quantum-correlated charm decays.

A. Li et al., arXiv:2610.15839, Sec. 2; BESIII, JHEP 06 (2025) 086. Phase vectors are schematic.

Outline

1. Physics motivation
2. Binned Dalitz formalism
3. Binning optimization
4. Results and validation
5. Summary and outlook

Fisher information and binning quality

Fit configuration: fixed hadronic inputs, only β floated

The Fisher information measures how strongly the event distribution changes with β:

$$I_\beta = N_{\text{sig}}\,\mathbb{E}\left[\left(\frac{\partial \ln p}{\partial \beta}\right)^2\right], \qquad \sigma_\beta \simeq I_\beta^{-1/2}.$$

The uncertainty relation is the large-sample limit for an efficient estimator.

Binning quality

$$Q^2 \equiv \frac{I_{\text{binned}}}{I_{\text{unbinned}}}.$$

Maximize the information retained.

Relative uncertainty reduction

$$g \equiv 1 - \frac{\sigma_{\text{opt}}}{\sigma_{\text{base}}} \simeq 1 - \frac{Q_{\text{base}}}{Q_{\text{opt}}}.$$

Compare at the same signal yield.

A. Li et al., arXiv:2610.15839, Sec. 3. The binning-independent denominator cancels in ratios of Q.

Time-integrated and time-dependent objectives

$$p_{ij}(t,q) \propto e^{-t/\tau_B}\left[U_{ij} + q(1-2\omega)\left(D_{ij}\cos\Delta m_B t + F_{ij}\sin\Delta m_B t\right)\right].$$

$q = +1/-1$: tagged as $B^0/\bar{B}^0$; $q = 0$: untagged; ω: mistag probability.
U_{ij}, D_{ij} describe the noninterfering terms; F_{ij} contains both $\sin 2\beta$ and $\cos 2\beta$.

Time-integrated method (TI)

$$Q^2_{\mathrm{TI}} \propto \frac{\sum_j k_j (c_j^2 + s_j^2)}{\sum_j k_j}.$$

Used for comparison: rewards large integrated interference. The B and D contributions factorize.

Time-dependent method (TD)

$$I_\beta = N_{\mathrm{sig}} \sum_{ijq} \int \mathrm{d}t \, \frac{(\partial_\beta p_{ij})^2}{p_{ij}}.$$

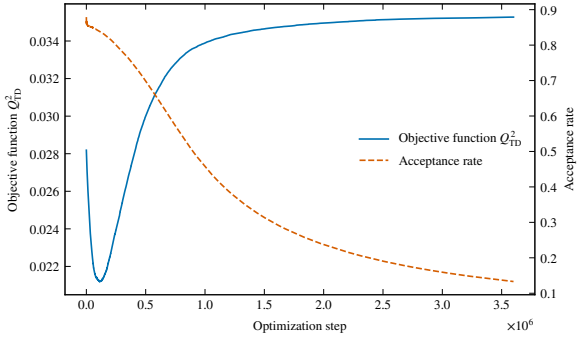
Used for the nominal binning: optimizes the β sensitivity with mixing and flavour tagging included.

Fit settings: $\beta = 22°$, $\omega = 0.36$, $0.3 < t < 14\,\mathrm{ps}$.

A. Li et al., arXiv:2610.15839, Eqs. (6), (15), (16). Only the B bin assignments are varied in both methods.

Simulated annealing

1. Start from equal-phase-difference bins.
2. Reassign a symmetric pair of Dalitz pixels.
3. Accept improvements; allow some losses while the temperature is high.
4. Cool gradually and retain the largest objective encountered.



Objective $\propto Q^2_{\mathrm{TD}}$; cumulative acceptance rate.

Ten runs with the same equal-phase initial binning and different random seeds: the spread in optimized expected uncertainties is below 0.01%.

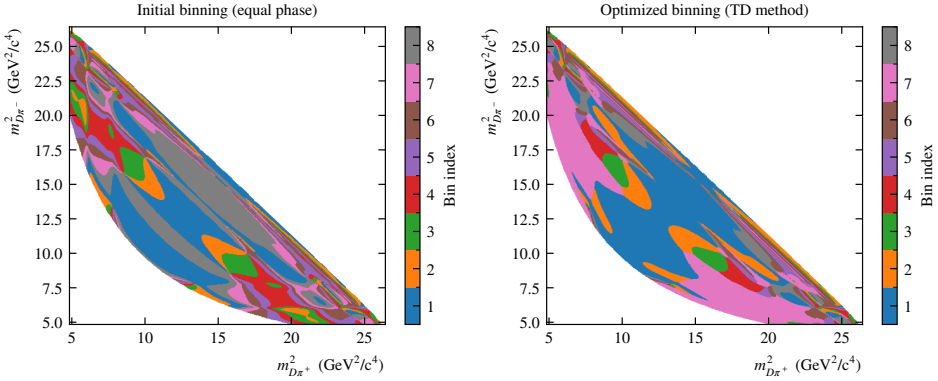
A. Li et al., arXiv:2610.15839, Secs. 3.3 and 4.1. Convergence-example settings: backup B4.

Outline

1. Physics motivation
2. Binned Dalitz formalism
3. Binning optimization
4. Results and validation
5. Summary and outlook

Optimized B-Dalitz binning

$\mathcal{M} = 8$ pairs: 16 bins symmetric under $\mu_+^2 \leftrightarrow \mu_-^2$.



Colour denotes $|j|$: a bin and its reflected partner share the same colour.

A. Li et al., arXiv:2610.15839, Fig. 3(b). Nominal TD optimization: uniform Dalitz efficiency, no smearing, no background.

Statistical sensitivity

Uncertainty reduction relative to equal-phase-difference binning.
Both evaluations use the same binned inputs without efficiency, smearing or background effects.

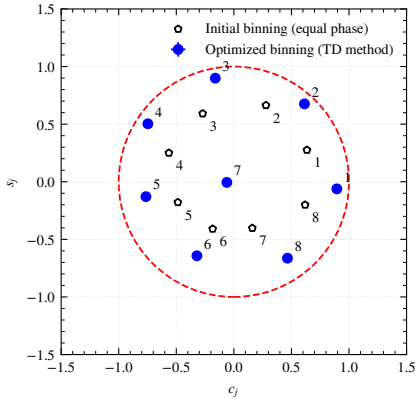
Binning scheme	TI evaluation	TD evaluation
TI-optimized	23.9%	5.0%
TD-optimized	13.4%	9.7%

The TI objective favours a different allocation of interference across bins. Its larger gain does not translate into the same gain in the β fit.

Optimizing the information in the time-dependent likelihood gives about a 10% smaller expected uncertainty on β.

A. Li et al., arXiv:2610.15839, Table 2. Fixed hadronic parameters; $g = 1 - Q_{\mathrm{base}}/Q_{\mathrm{opt}}$.

Optimized strong-phase parameters



Reading the strong-phase parameters

- Each point is one positive-index bin; the dashed circle is $c_j^2 + s_j^2 = 1$.
- Most optimized points move towards the circle.
- Bin 7 lies near the origin: this selected scheme groups much of the low-sensitivity region together.

The total information matters. A large interference magnitude in every bin is not required.

A. Li et al., arXiv:2610.15839, Fig. 4(b) and Sec. 4.1. Paired bins obey $c_{-j} = c_j$, $s_{-j} = -s_j$.

Toy Monte Carlo validation

Signal-only toy fits

- About $13\,000$ signal events per pseudoexperiment.
- 250 pseudoexperiments generated per configuration.
- Only β floated; hadronic inputs fixed.
- No efficiency or resolution effects.

Mean fit-reported uncertainty

Binning	$\overline{\sigma}_\beta$
Equal phase	$(4.886 \pm 0.027)^\circ$
TD-optimized	$(4.433 \pm 0.022)^\circ$

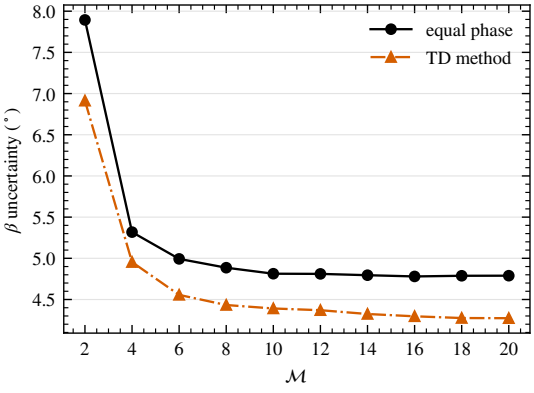
Errors on the ensemble means are statistical. The signal yield is assumed for this study.

Predicted reduction: 9.7%. Toy result: $(9.3 \pm 0.7)\%$.

Ensemble means use accepted fits, with valid minima, accurate covariance matrices and $|\mathrm{pull}_\beta| \leq 8$.

A. Li et al., arXiv:2610.15839, Tables 4–5. $\beta_{\mathrm{gen}} = 22^\circ$, $\omega = 0.36$; identical nominal optimized map throughout.

Dependence on the number of bins



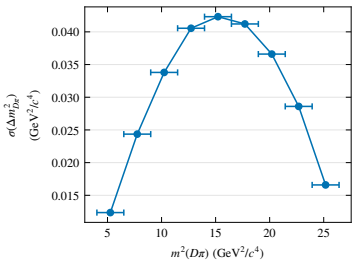
$\mathcal{M}$ counts pairs; there are $2\mathcal{M}$ bins

- Rapid improvement up to about $\mathcal{M} = 8$.
- Larger $\mathcal{M}$ gives small, nonmonotonic changes.
- More bins leave fewer events to constrain each hadronic input.

Nominal choice: 16 bins.

A. Li et al., arXiv:2610.15839, Fig. 6. Mean fit-reported uncertainties; about $13\,000$ signal events; no efficiency effects; hadronic inputs fixed.

Dalitz-plot resolution



Representative resolution in each $m^2(D\pi)$ coordinate.

Toy uncertainty reduction

B Dalitz resolution	Improvement
Not included	$(9.3 \pm 0.7)\%$
Included	$(9.4 \pm 0.7)\%$

The absolute uncertainties increase by about 2% in both binnings. The corresponding Q_{TD} predictions are 9.68% and 9.66%.

For this response model, migration across bins leaves the relative sensitivity gain statistically unchanged.

A. Li et al., arXiv:2610.15839, Fig. 9 and Table 4. The fixed nominal map is evaluated with and without smearing; no other experimental effects.

Efficiency and background studies

Effect studied	Reported comparison
Decay-time acceptance	Applying a common time acceptance in evaluation leaves the nominal 9.7% gain unchanged at the quoted precision.
Dalitz efficiency	Evaluating the fixed nominal map with representative nonuniform efficiency changes the prediction from 9.7% to 11.6%.
Background	Including background in the optimization changes the subsequent signal-only gain by about two percentage points at $f_{\mathrm{sig}} = 0.8$.

The gain remains about 10% with the tested efficiencies. Including background in optimization changes the signal-only gain by about two percentage points.

A. Li et al., arXiv:2610.15839, Sec. 4.2. Efficiency and background configurations are detailed in backups B5–B6.

Outline

1. Physics motivation
2. Binned Dalitz formalism
3. Binning optimization
4. Results and validation
5. Summary and outlook

Using the published binning

Binning supplied by this work

- Nominal TD-optimized B scheme: $\mathcal{M} = 8$ pairs, 16 bins.
- Use the supplied bin definitions and code to assign the B-bin index j to each event.
- The established D binning gives the index i.

Measuring β with data

- Fit the B hadronic parameters together with β, using D_{CP} modes if needed.
- Use measured D strong-phase inputs with their uncertainties and correlations.
- Include efficiency, resolution, flavour tagging and background in the likelihood.

Use the published binning directly in the measurement, with hadronic inputs determined from data.

Bin definitions and code: A. Li et al., arXiv:2610.15839, ancillary files. Fit method: Bondar, Kuzmin, Vorobyev, JHEP 03 (2018) 195.
D_{CP}: D in a CP eigenstate.

Summary

About 10% smaller statistical uncertainty

at the same signal yield, with hadronic parameters fixed in the fits.

1. Use the Fisher information of the **time-dependent β likelihood** to choose the bins.
2. The nominal **16-bin symmetric scheme** predicts 9.7% improvement; toys give $(9.3 \pm 0.7)\%$ without experimental effects.
3. The optimized binning retains a sensitivity advantage under the experimental conditions studied.

At $\sigma \propto N^{-1/2}$, a 10% uncertainty reduction corresponds to about 23% more events with the baseline binning.

Paper and machine-readable bin definitions: arXiv:2610.15839

B1 Time-dependent decay rate

$$p_{ij}(t,q) \propto e^{-t/\tau_B}\left[U_{ij} + q(1-2\omega)\{D_{ij}\cos(\Delta m_B t) + F_{ij}\sin(\Delta m_B t)\}\right],$$

$$\begin{aligned} U_{ij} &= \tfrac{1}{2}(K_{-i}k_j + K_i k_{-j}), \\ D_{ij} &= \tfrac{1}{2}(K_{-i}k_j - K_i k_{-j}), \\ F_{ij} &= -\sqrt{K_i K_{-i} k_j k_{-j}}\left[(C_i s_j - S_i c_j)\cos 2\beta - (C_i c_j + S_i s_j)\sin 2\beta\right]. \end{aligned}$$

- $q = +1/-1$ for a $B^0/\bar{B}^0$ tag, $q = 0$ if untagged; ω is the mistag probability.
- Positive proper time $t \geq 0$ is used here. A B factory uses signed Δt and $e^{-|\Delta t|/\tau_B}$.
- Leading $b \to c\bar{u}d$ amplitudes; charm mixing and direct charm CP violation are neglected.

A. Li et al., arXiv:2610.15839, Sec. 2; Bondar, Kuzmin, Vorobyev, JHEP 03 (2018) 195. The corresponding subleading effects require consideration in a precision measurement.

B2 Hadronic parameters and bin weights

Write $S\Phi = (\mu_-^2, \mu_+^2)$ for coordinate exchange:

$$\bar{A}_B(\Phi) = A_B(S\Phi), \qquad S\mathcal{B}_j = \mathcal{B}_{-j}.$$

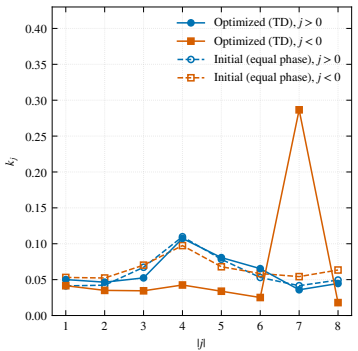
$$c_j + i s_j = \frac{\int_{\mathcal{B}_j} A_B^*(\Phi) A_B(S\Phi)\,\mathrm{d}\Phi}{\sqrt{k_j k_{-j}}}.$$

$$c_{-j} = c_j, \quad s_{-j} = -s_j, \quad c_j^2 + s_j^2 \le 1.$$

D parameters obey analogous relations.

$$k_j = \int_{\mathcal{B}_j} |A_B(\Phi)|^2\,\mathrm{d}\Phi, \qquad \sum_j k_j = 1.$$

Bin weights also affect the sensitivity.



Nominal TD scheme: initial and optimized k_j for both signs of the bin index.

A. Li et al., arXiv:2610.15839, Sec. 2 and Fig. 5(b). The displayed normalization is a convention for the hadronic integrals.

B3 Nuisance parameters and profiled information

Let $\theta = (\beta, h)$, with h the hadronic and experimental nuisance parameters:

$$I(\theta) = \begin{pmatrix} I_{\beta\beta} & I_{\beta h} \\ I_{h\beta} & I_{hh} \end{pmatrix}.$$

Fixed h: the fit considered here

$$\sigma_\beta^2 \gtrsim \frac{1}{I_{\beta\beta}}.$$

The objective measures sensitivity with the hadronic inputs known.

Profiled h: an experimental fit

$$\sigma_\beta^2 \gtrsim (I^{-1})_{\beta\beta} = \frac{1}{I_{\text{eff}}},$$

$$I_{\text{eff}} = I_{\beta\beta} - I_{\beta h} I_{hh}^{-1} I_{h\beta}.$$

External constraints and additional decay modes can reduce the loss from nuisance-parameter correlations. The resulting optimal binning should be assessed in that joint fit.

Fixed-input scope: A. Li et al., arXiv:2610.15839, Sec. 3. The block-matrix expression is the Schur complement for an invertible nuisance block.

B4 Annealing configuration and convergence

For a positive objective, define

$$\delta_{\mathrm{rel}} = \frac{Q^2_{\mathrm{new}} - Q^2_{\mathrm{old}}}{Q^2_{\mathrm{old}}}, \qquad P_{\mathrm{accept}} = \min\left(1, e^{\delta_{\mathrm{rel}}/T}\right) \quad (T > 0).$$

At $T = 0$, accept $\delta_{\mathrm{rel}} \geq 0$ and reject losses.

Run settings

Configuration	T_0	N_{total}	k
TI	2×10^{-5}	2.4×10^{7}	20
TD, signal only	10^{-4}	4.32×10^{6}	25
TD, background	5×10^{-6}	1.68×10^{6}	50

Cooling and proposals

$$T = T_0 \left[1 - \frac{n}{N_{\mathrm{total}} - 1}\right]^k.$$

$n = 0, \ldots, N_{\mathrm{total}} - 1.$

- 60% uniform label draws; 40% ± 1 shifts.
- No spatial-connectivity constraint.

A. Li et al., arXiv:2610.15839, Table 1. The plotted convergence example uses $N_{\mathrm{total}} = 3.6 \times 10^6$, $T_0 = 10^{-4}$, $k = 25$.

B5 Efficiency configurations

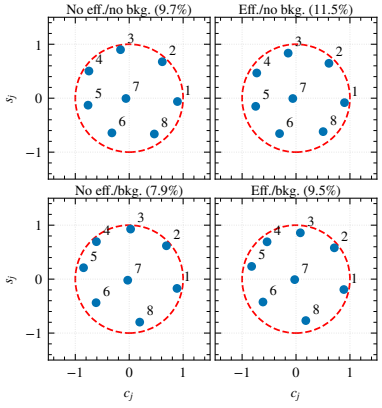
Predicted uncertainty reduction (%); ε_t: time acceptance, $\varepsilon_{\mathrm{DP}}$: Dalitz efficiency.

In optimization		In evaluation			
ε_t	$\varepsilon_{\mathrm{DP}}$	Neither	ε_t	$\varepsilon_{\mathrm{DP}}$	Both
No	No	9.7	9.7	11.6	11.6
Yes	No	9.7	9.7	11.6	11.6
No	Yes	9.0	9.0	11.0	11.0
Yes	Yes	9.6	9.6	11.5	11.5

- Nominal map, with experimental effects: Q predicts 11.6%; toys give $(11.1 \pm 0.7)\%$.
- The combined comparison does not isolate each individual response effect.
- With exchange-asymmetric efficiency, conjugate-bin integrals require separate treatment.

A. Li et al., arXiv:2610.15839, Tables 3 and 5. Efficiencies are representative assumptions; all quoted fits hold hadronic inputs fixed.

B6 Background-dependent optimization



Optimization PDF

$$p = f_{\mathrm{sig}} p_{\mathrm{sig}} + (1 - f_{\mathrm{sig}}) p_{\mathrm{bkg}}, \qquad f_{\mathrm{sig}} = 0.8.$$

Subsequent evaluation

Each map is evaluated with the background-free Q_{TD} and its matching efficiency configuration.

- No efficiency: $9.7\% \to 7.9\%$.
- With efficiency: $11.5\% \to 9.5\%$.

These are signal-only reevaluations of maps found with background.

A. Li et al., arXiv:2610.15839, Fig. 12. The efficiency-optimized reference here is distinct from the fixed nominal-map evaluation giving 11.6%.

B7 Previous measurements of β

- **Belle (2016):** a model-independent, binned D Dalitz analysis of $B^0 \to D^{(*)}h^0$ with external strong-phase information.
- **BaBar + Belle (2018):** a D-amplitude-model analysis of $B^0 \to D^{(*)}h^0$ resolved the $\beta \leftrightarrow \pi/2 - \beta$ ambiguity at more than 5σ.
- **Bondar, Kuzmin, Vorobyev (2018):** the binned double-Dalitz method for $B^0 \to D\pi^+\pi^-$, including joint use of D_{CP} channels.

The present contribution is the dedicated B-Dalitz binning optimization for the time-dependent β measurement.

Belle, Phys. Rev. D 94 (2016) 052004; BaBar + Belle, Phys. Rev. Lett. 121 (2018) 261801; Bondar, Kuzmin, Vorobyev, JHEP 03 (2018) 195.

B8 References and bin definitions

1. **This study:** A. Li, W. Qian, B. Shi, A. Xu and L. Zhang, arXiv:2610.15839. Machine-readable bin grid, axis definitions and Python reader are available as ancillary files.

2. **Double-Dalitz β method:** A. Bondar, A. Kuzmin and V. Vorobyev, JHEP 03 (2018) 195, arXiv:1802.00200.

3. **B amplitude model:** LHCb Collaboration, Phys. Rev. D 92 (2015) 032002, arXiv:1505.01710.

4. **Related double-Dalitz optimization for γ:** D. C. Craik, T. Gershon and A. Poluektov, Phys. Rev. D 97 (2018) 056002, arXiv:1712.07853.

5. **Measured charm strong phases:** BESIII Collaboration, JHEP 06 (2025) 086, arXiv:2503.22126.